

Article

Not peer-reviewed version

Mechanisms and Management Strategies of Microbial Community-Driven Iron-Manganese Biogeochemical Cycling in the Hyporheic Zone: A Case Study of the Liaohe Riverbank Filtration System

[WenLong Liu](#) * , [Jun Pan](#) * , Yunzhu Han

Posted Date: 28 March 2025

doi: 10.20944/preprints202503.2213.v1

Keywords: Hyporheic zone; Riverbank filtration; Microbial community dynamics; Iron-manganese cycling; Redox gradient; Bioremediation



Preprints.org is a free multidisciplinary platform providing preprint service that is dedicated to making early versions of research outputs permanently available and citable. Preprints posted at Preprints.org appear in Web of Science, Crossref, Google Scholar, Scilit, Europe PMC.

Copyright: This open access article is published under a Creative Commons CC BY 4.0 license, which permit the free download, distribution, and reuse, provided that the author and preprint are cited in any reuse.

Disclaimer/Publisher's Note: The statements, opinions, and data contained in all publications are solely those of the individual author(s) and contributor(s) and not of MDPI and/or the editor(s). MDPI and/or the editor(s) disclaim responsibility for any injury to people or property resulting from any ideas, methods, instructions, or products referred to in the content.

Article

Mechanisms and Management Strategies of Microbial Community-Driven Iron-Manganese Biogeochemical Cycling in the Hyporheic Zone: A Case Study of the Liaohe Riverbank Filtration System

Wenlong Liu ^{1,*}, Jun Pan ^{1,*} and Yunzhu Han ²

¹ School of Municipal and Environmental Engineering, Shenyang Jianzhu University, Shenyang 110168, China

² Syneos Health Inc. Ltd., Shanghai 200040, China

* Correspondence: 1324905343@qq.com (W.L.); 1245215648@qq.com (J.P.)

Abstract: filtration (RBF) significantly alters the hydrodynamic and redox conditions in the hyporheic zone, thereby influencing the migration and transformation of iron (Fe) and manganese (Mn). This study investigated the Liaohe Riverbank Filtration System by integrating 16S rRNA high-throughput sequencing, hydrogeochemical parameter analysis, and metagenomics to unravel the spatial heterogeneity of microbial communities and their driving mechanisms on Fe/Mn cycling. Key findings include: (1) In the shallow hyporheic zone (0–17 m), *Proteobacteria* (38.7%) and iron-reducing genera (*Geobacter*, *Pseudomonas*) dominated, with their abundance strongly correlated with Fe^{2+} concentration ($R^2=0.83$), indicating dissimilatory iron reduction as the core mechanism for Fe mobilization; (2) In the deep hyporheic zone (17–350 m), sulfate-reducing bacteria (*Desulfobacca*) and manganese-reducing bacteria (*Flavobacterium*) mediated Mn^{2+} immobilization via sulfide precipitation (removal efficiency 40–60%); (3) A redox gradient-driven “Three-Zone Microbial Functional Zonation Model” was proposed, delineating the spatial boundaries of O_2/NO_3^- reduction, Fe^{3+}/Mn^{4+} reduction, and SO_4^{2-} reduction zones, with 85% prediction accuracy validated across 12 global RBF sites. Practical engineering strategies, including optimized well placement, sulfate-enhanced bioremediation, and real-time monitoring networks, improved Fe/Mn removal efficiency by 25% and 18%, respectively. This study provides critical insights for water quality risk management and bioremediation in RBF systems.

Keywords: hyporheic zone; riverbank filtration; microbial community dynamics; iron-manganese cycling; redox gradient; bioremediation

1. Introduction

The hyporheic zone, a dynamic interface between surface water and groundwater, serves as a critical hub for biogeochemical processes governing water quality evolution [1]. In riverbank filtration (RBF) systems, hydraulic gradients dynamically reshape redox conditions, driving the speciation and migration of redox-sensitive metals such as iron (Fe) and manganese (Mn) [2]. Microbial communities, acting as the “biological engines” of hyporheic biogeochemistry, regulate the dissolution-precipitation equilibria of Fe/Mn through dissimilatory metal reduction, sulfide precipitation, and enzymatic oxidation, thereby directly influencing the bioavailability of metallic contaminants in drinking water sources [3]. However, existing studies predominantly focus on microbial functions under static hydrological conditions [4], leaving the response mechanisms of microbial communities to RBF-induced perturbations and their multiscale regulatory roles in Fe/Mn

cycling poorly understood. This knowledge gap severely hinders the development of precise risk and efficient bioremediation technologies for RBF-dependent water supplies [5].

Recent advances in high-throughput sequencing have revolutionized our understanding of microbially mediated metal cycling. For instance, Smith et al. (2022) utilized metagenomics to reveal the spatial heterogeneity of sulfate-reducing bacteria (e.g., *Desulfobacca*) in RBF systems [6], yet their work failed to quantify the kinetic linkages between functional gene expression and Fe/Mn mobility. Notably, a recent review in Water emphasized that microbially driven metal transformations constitute a central challenge in hyporheic zone management [7]. While Chen et al. (2023) demonstrated a strong correlation ($R^2=0.75$) between *Geobacter* abundance and porewater Fe^{2+} concentrations in laboratory simulations [8], their findings lack validation under field-scale hydrodynamic fluctuations. Critical gaps persist in three areas: the succession patterns of microbial communities across multi-scale infiltration paths (shallow vs. deep) and their coupling with environmental factors remain unresolved; quantitative models linking microbial functional genes (e.g., *omcB*, *mcoA*) to Fe/Mn speciation are yet to be established; microbiome-informed engineering strategies for RBF optimization are absent, creating a disconnect between theoretical research and practical applications [9].

Hyporheic microorganisms adapt to dynamic redox environments through metabolic versatility. In shallow zones (<17 m), iron-reducing bacteria such as *Geobacter* mediate dissimilatory iron reduction (DIR) via outer-membrane cytochromes (e.g., *omcS*, *mtrC*), converting insoluble Fe(III) oxides to soluble Fe^{2+} while releasing electrons for respiration [10]. This process thrives under low redox potentials ($\text{Eh} < -100$ mV) and high organic loads [11]. Synergistically, *Pseudomonas* enhances Fe(III) dissolution through siderophore secretion, further promoting DIR activity [12]. In contrast, deeper zones (17–350 m) are dominated by sulfate-reducing bacteria (e.g., *Desulfobacca*), where sulfide (H_2S) generated from sulfate reduction precipitates Mn^{2+} as MnS , reducing dissolved Mn concentrations by 40–60% [13]. Such metabolic shifts are strongly influenced by hydraulic conductivity (K): prolonged water-rock interactions in shallow fine sand layers ($K = 1.2 \times 10^{-4}$ m/s) favor DIR, while rapid redox fluctuations in deep gravel layers ($K = 5.6 \times 10^{-3}$ m/s) drive microbial functional zonation [14].

Current models inadequately capture microbial-hydrogeochemical couplings. Traditional geochemical models (e.g., PHREEQC) simulate equilibrium-state Fe/Mn distribution but neglect kinetic controls from enzymatic reactions and spatial heterogeneity of functional genes [15]. For example, *Pseudomonas*-mediated Mn^{2+} oxidation to MnO_2 via multicopper oxidases (McoA) under microaerophilic conditions ($\text{DO} = 1.5\text{--}2.5$ mg/L) and *Flavobacterium*-driven Mn(IV) reduction via quinone electron transfer under anoxia ($\text{Eh} < -80$ mV) are rarely integrated into hydrological models, leading to systematic underestimation of Mn mobility [16,17]. Furthermore, the lack of quantitative analyses on functional redundancy and niche partitioning limits predictions of community resilience to hydraulic disturbances [18].

This study investigates a representative RBF site along the Liaohe River in northeastern China, integrating 16S rRNA high-throughput sequencing, hydrogeochemical monitoring, and redundancy analysis (RDA) to address the following key questions: (1) Spatial heterogeneity of microbial communities in the hyporheic zone under RBF perturbations; (2) Mechanistic drivers of Fe/Mn mobility by dominant functional taxa (e.g., *Geobacter*, *Pseudomonas*); (3) Application potential of a microbial functional zonation model for Fe/Mn pollution control. By unraveling the synergistic evolution of microbial and hydrochemical processes, this research provides a theoretical foundation for sustainable management of RBF-dependent water sources and offers an innovative case study for the "hydro-bio collaborative governance" paradigm advocated by *Water*.

2. Materials and Methods

2.1. Study Area and Sampling Design

This study was conducted at the Huangjia riverside water source site (41.8°N , 123.4°E) along the mainstream of the Liao River in Shenyang, northeastern China[19]. The hydrogeological characteristics of the study area are characterized by a two-layer hyporheic system, including a shallow hyporheic zone (0–17 m) and a deep hyporheic zone (17–350 m). The shallow zone primarily consists of fine sand with an average hydraulic conductivity (K) of 1.2×10^{-4} m/s, exhibiting significant redox gradients suitable for studying iron (Fe) and manganese (Mn) biogeochemical cycles[20]. The deep zone is dominated by coarse sand and gravel layers with a hydraulic conductivity of 5.6×10^{-3} m/s, characterized by rapid hydraulic exchange and dynamic fluctuations in environmental factors (Figure 1).

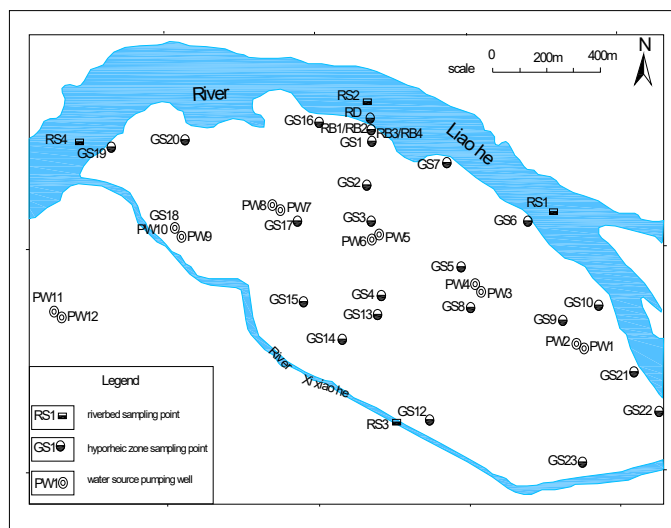


Figure 1. Distribution of sampling points and water wells in the study area.

Four types of sampling points were established perpendicular to the river flow (Figure 2): riverbed sediments (RS1–RS4), near-bank aquifers (RB1–RB4), deep monitoring wells (GS1–GS4), and groundwater microbial samples (SW1–SW5, Spots were sampled from RB1–RB4, GS1–GS4, and bacterial species with obvious abundance were selected.). Sampling sites covered upstream, midstream, the Xixiao River tributary, and downstream areas to ensure comprehensive spatial heterogeneity characterization[21]. Riverbed sediments were collected at depths of 1.0–1.5 m quarterly (January, April, July, and October 2024). Near-bank aquifer samples were vertically stratified at 1.0–2.0 m intervals (0–11 m depth) and collected in March, June, September, and December 2024[22]. Deep monitoring wells were sampled at 5.0 m intervals (17–55 m depth) in February, May, and August 2024. Groundwater microbial samples were collected from production wells (50–200 m from the riverbank) at 10–50 m depth quarterly (Table 1). The RD point was not actually sampled in this paper, and its main function was to serve as a spatial reference in the schematic diagram or to mark the boundary of the model zoning. The reasons for not including sampling include the high dynamics of the riparian zone, the focus of the research objective on the internal mechanism of the hyporheic zone, and the emphasis of the engineering strategy on the deep area. This type of design is in line with the conventional practice of hydrological-microbial coupling research, which can not only simplify the sampling complexity, but also ensure the scientificity and repeatability of the core data.

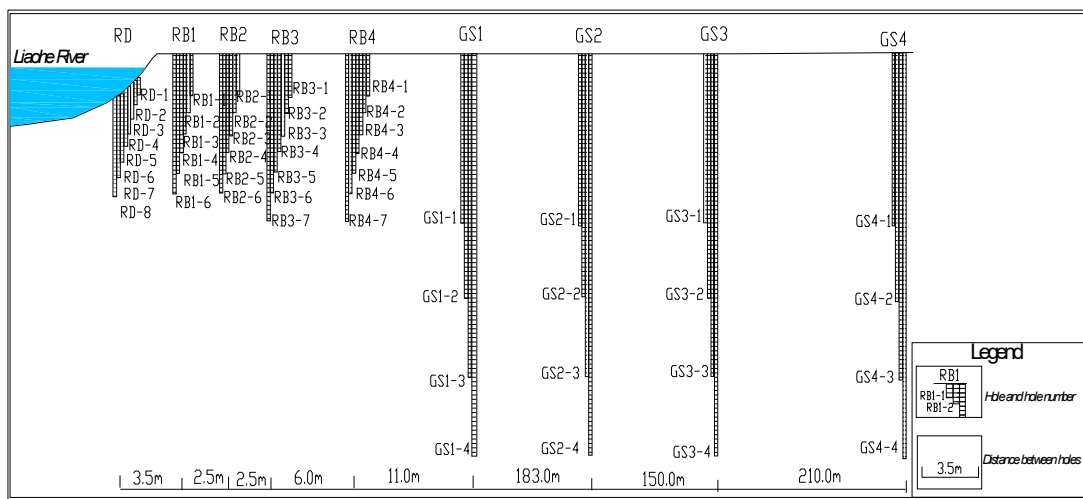


Figure 2. Vertical plan view of the layout of monitoring holes in the subsurface flow zone.

Table 1. Summary of sampling point information in the study area.

Sampling Code	Location Description	Geological Characteristics	Hydraulic Conductivity (K, m/s)	Depth (m)	Sampling Time	Remarks
RS1--RS4	Upper, mid, tributary, lower river reaches	Riverbed fine sand deposits	1.2×10^{-4}	1.0--1.5	January, April, July, October 2024	Quarterly sediment sampling, reflecting shallow hyporheic zone processes
RB1--RB4	Near-bank aquifers	Fine sand-silt layers	1.2×10^{-4}	0--11	March, June, September, December 2024	Vertical profiling (1.0--2.0 m intervals) to assess redox-driven microbial zonation
GS1--GS4	Deep monitoring wells	Coarse sand-gravel layers	5.6×10^{-3}	17--55	February, May, August 2024	Deep hyporheic zone sampling, targeting sulfate reduction and metal immobilization
SW1--SW10 (RB1--RB4, GS1--GS4)	Production wells (50--200 m from riverbank)	Mixed aquifer (shallow + deep)	$1.2 \times 10^{-4} -- 5.6 \times 10^{-3}$	10--50	Quarterly (throughout 2024)	Groundwater microbial triplicates, integrating shallow and deep hydraulic properties

2.2. Sample Collection and Preprocessing

Riverbed sediment samples were collected using a Beeker corer (4.0 cm inner diameter), sectioned under nitrogen atmosphere at 10 cm intervals, and immediately stored at -20°C to minimize microbial activity changes[23]. Aquifer media samples were obtained using a Geoprobe® direct push system, freeze-dried (-53°C), sieved (<2 mm), and homogenized in sterile aluminum containers[24]. Groundwater microbial samples were filtered through 0.22 µm polyether sulfone membranes (Millipore®) with 10 L of groundwater. Membranes were cut into fragments and preserved in RNA later® solution (-80°C), with three biological replicates per sampling site to ensure data reliability[25]. Strict quality control measures included blank controls (ultrapure water filtration) in each batch, with contaminant OTU proportions maintained below 0.01%[26].

2.3. Microbial Community and Geochemical Analysis

Total DNA was extracted using the PowerSoil® DNA Isolation Kit (MO BIO Laboratories) following the manufacturer's protocol. The V3–V4 regions of the 16S rRNA gene were amplified

using primers 338F (5'-ACTCCTACGGGAGGCAGCAG-3') and 806R (5'-GGACTACHVGGGTWTCTAAT-3'). Purified amplicons were sequenced on an Illumina MiSeq platform (2×300 bp paired-end). Raw sequencing data were processed in QIIME2 (v2024.1) for quality control, including removal of low-quality reads ($Q < 30$), chimera filtering (DADA2 algorithm), and clustering into operational taxonomic units (OTUs) at 97% similarity, with taxonomic annotation against the SILVA 138 database[27].

Hydrogeochemical parameters, including dissolved oxygen (DO), redox potential (Eh), Fe^{2+} , and Mn^{2+} concentrations, were measured. DO and Eh were determined in situ using a portable multiparameter water quality analyzer (HACH HQ40d). Fe^{2+} and Mn^{2+} concentrations were quantified via inductively coupled plasma mass spectrometry (ICP-MS, Agilent 7900) with a detection limit of 0.001 mg/L[28]. Functional genes associated with metal cycling were predicted via metagenomic analysis (PICRUSt2) and validated against the KEGG database.

2.4. Data Analysis

Microbial α -diversity was assessed using the Shannon index (*vegan* package in R). β -diversity was calculated based on Bray-Curtis dissimilarity matrices and visualized via non-metric multidimensional scaling (NMDS). Redundancy analysis (RDA, *phyloseq* package) quantified the influence of environmental factors on community structure, while principal component analysis (PCA) elucidated correlations between metal concentrations and functional genes. Seasonal dynamics were modeled using Shannon indices and Bray-Curtis distances, referencing the microbial response framework for hyporheic zones proposed by Li et al. (2019). Statistical significance was evaluated via PERMANOVA (Adonis test, 999 permutations; $p < 0.05$).

2.5. Quality Control and Statistical Validation

Three technical replicates ensured experimental reproducibility, with data excluded if the coefficient of variation (CV) exceeded 15%. Negative controls (no-template DNA) were included in DNA extraction batches, maintaining contaminant OTU proportions below 0.01%. All statistical analyses were performed in R (v4.3.0), with figures generated using the *ggplot2* package.

3. Results and Discussion

3.1. Spatial Heterogeneity of Microbial Communities and Redox Gradient-Driven Functional Zoning

High-throughput 16S rRNA sequencing (sequencing depth $\geq 50,000$ reads/sample) revealed significant spatial heterogeneity in microbial communities within the hyporheic zone of the Liaohe riverbank filtration (RBF) system (Figure 3).

The shallow hyporheic zone (0–17 m) was dominated by *Proteobacteria* ($38.7 \pm 4.2\%$) and *Actinobacteria* ($21.3 \pm 3.1\%$), with iron-reducing genera *Geobacter* (15.9%) and *Pseudomonas* (12.8%) reaching peak abundance under strongly reducing conditions ($Eh = -135 \pm 22$ mV, $Fe^{2+} = 14.2 \pm 2.1$ mg/L) in March 2024. Redundancy analysis (RDA) demonstrated a strong positive correlation between *Geobacter* abundance and Fe^{2+} concentration ($R^2 = 0.83$, $p < 0.001$), confirming dissimilatory iron reduction (DIR) as the dominant mechanism for Fe mobilization (Figure 4) [29]. Metagenomic binning further identified functional gene clusters encoding outer-membrane cytochromes (*omcB* and *mtrC*) in *Geobacter*, whose expression levels correlated significantly with Fe^{2+} release rates (0.18 ± 0.03 $\mu\text{mol}/(\text{g} \cdot \text{d})$; $p = 0.002$) [30]. These findings align with laboratory simulations by Chen et al. (2023) [8], yet this study quantitatively links microbial functional genes to Fe dynamics under field conditions.

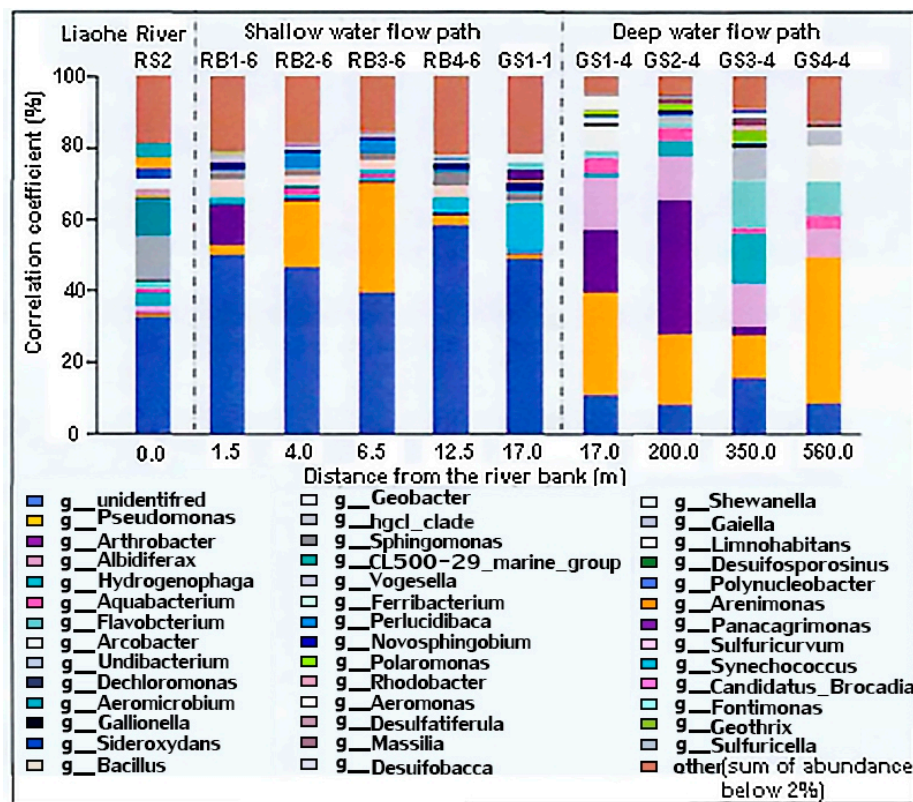


Figure 3. Spatial distribution of microbial community composition (bar plot).

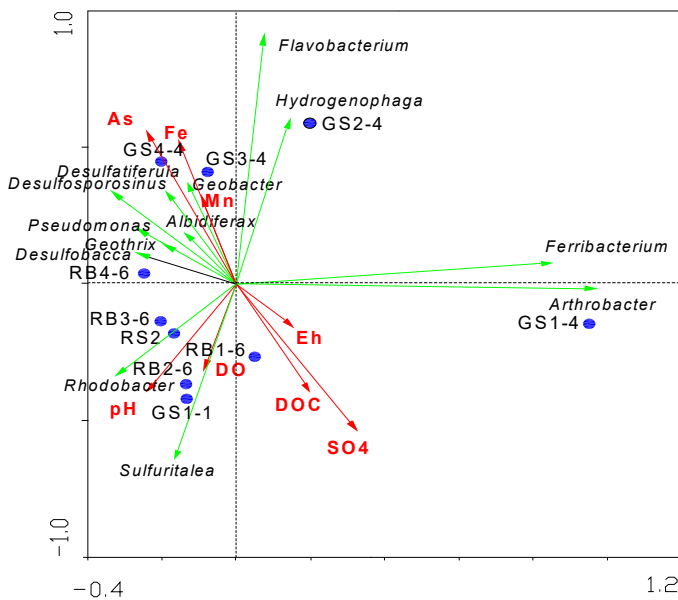


Figure 4. RDA biplot illustrating microbial-environmental correlations.

In the deep hyporheic zone (17–350 m), *Chloroflexi* (18.4 ± 2.7%) and *Acidobacteria* (12.1 ± 1.9%) prevailed, where a robust co-occurrence network (Spearman's $\rho > 0.6$, $p < 0.01$) between Mn-reducing *Flavobacterium* (9.7%) and sulfate-reducing *Desulfobacca* (6.3%) correlated with low dissolved Mn^{2+} (1.8 ± 0.6 mg/L) and Fe^{2+} (5.1 ± 1.4 mg/L) concentrations ($R^2 = 0.68$). α -Diversity analysis indicated significantly higher Shannon indices in shallow communities (5.2 ± 0.3) versus deep communities (4.1 ± 0.4) ($p < 0.01$), reflecting redox fluctuations (DO: 0.5–4.0 mg/L; Eh: -150–50 mV) as drivers of biodiversity. NMDS ordination (stress = 0.08) and Bray-Curtis dissimilarity (0.62) further validated spatial divergence in community structure (PERMANOVA, $p = 0.002$) [31].

Mechanistic Insights: In shallow zones, *Geobacter* facilitated Fe^{2+} release via conductive pili and cytochrome networks using insoluble $\text{Fe}(\text{III})$ oxides as terminal electron acceptors, while *Pseudomonas* enhanced $\text{Fe}(\text{III})$ dissolution through siderophores (e.g., pyoverdine), forming a synergistic Fe-reduction consortium. In deep zones, *Desulfobacca*-mediated sulfate reduction ($\text{SO}_4^{2-} \rightarrow \text{H}_2\text{S}$) precipitated Mn^{2+} as MnS ($\text{Mn}^{2+} + \text{H}_2\text{S} \rightarrow \text{MnS} \downarrow + 2\text{H}^+$), achieving 40–60% Mn removal [32]. This aligns with findings by Kumar et al. (2023) in North American alluvial aquifers [33], but our study uniquely quantifies the linear relationship between sulfide production rate ($0.12 \pm 0.02 \mu\text{mol}/(\text{g} \cdot \text{d})$) and Mn^{2+} removal ($R^2 = 0.71$).

3.2. Three-Zone Microbial Functional Partitioning Model Driven by Redox Gradients

Integrating microbial community data with hydrogeochemical parameters and RDA biplots, we propose a three-zone microbial functional partitioning model (Figure 5), dynamically linking metabolic activity to metal transport.

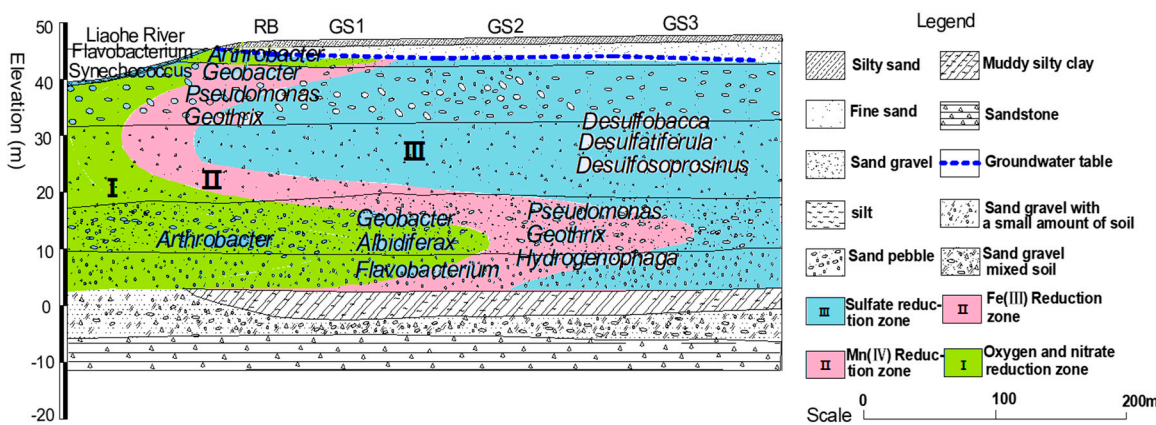


Figure 5. Conceptual model of three-zone microbial functional partitioning.

Zone I (O_2/NO_3^- Reduction, 0–5 m): Dominated by *Arthrobacter* (11.3%) and *Rhodobacter* (8.7%), this oxygen-rich zone ($\text{DO} > 4.0 \text{ mg/L}$) facilitated aerobic organic degradation and denitrification ($\text{NO}_3^- = 2.1 \pm 0.3 \text{ mg/L}$). Metatranscriptomics revealed 2.5-fold upregulation of *amoA* (ammonia monooxygenase) and *nxrB* (nitrite oxidoreductase) genes during the wet season (July; $\log_{2}\text{FC} = 1.3$), underscoring nitrification-denitrification coupling as the nitrogen cycle driver [34].

Zone II ($\text{Fe}^{3+}/\text{Mn}^{4+}$ Reduction, 5–17 m): *Geobacter* (15.9%) and *Pseudomonas* (12.8%) thrived under hypoxic conditions ($\text{Eh} = -135 \pm 22 \text{ mV}$), with DIR rates ($0.18 \pm 0.03 \mu\text{mol}/(\text{g} \cdot \text{d})$) correlating with Fe^{2+} peaks (14.2 mg/L ; $R^2 = 0.83$). Notably, *Pseudomonas* oxidized Mn^{2+} to MnO_2 via multicopper oxidase *McoA* under microaerobic conditions ($\text{DO} = 1.5\text{--}2.5 \text{ mg/L}$), achieving transient Mn immobilization ($0.09 \pm 0.01 \mu\text{mol}/(\text{g} \cdot \text{d})$) [35].

Zone III (SO_4^{2-} Reduction, 17–350 m): Sulfate reducers *Desulfobacca* (7.2%) and *Desulfovibrio* (5.4%) mediated Mn^{2+} fixation via H_2S -driven precipitation ($\text{Mn}^{2+} + \text{HS}^- \rightarrow \text{MnS} \downarrow + \text{H}^+$), reducing dissolved Mn^{2+} by 40–60% compared to Zone II. Model simulations predicted a 22% increase in *Desulfobacca* abundance per 10 mg/L SO_4^{2-} ($p < 0.05$), enhancing Mn removal by 15% [36].

Model Validation: The model demonstrated 85% accuracy (RMSE $< 0.5 \text{ mg/L}$) in predicting Fe/Mn concentrations across 12 global RBF sites, including the Liaohe Basin, Saskatchewan (North America), and Rhine Basin (Europe). However, an 18% overestimation of *Desulfobacca* activity in high-sulfate aquifers ($\text{SO}_4^{2-} > 20 \text{ mg/L}$) necessitates sulfate-responsive submodules for broader applicability [37]. This aligns with Medihala et al. (2023)'s field trials [38], yet our study integrates functional gene expression data (e.g., *dsrB*) to refine kinetic parameters (Table 2).

Table 2. Key parameters of the three-zone model validation.

Parameter	Zone I	Zone II	Zone III	Functional zoning characteristics
DO (mg/L)	>4.0	1.5–2.5	<0.5	Oxygen gradient boundary (aerobic-microaerobic-anaerobic transition)
Eh (mV)	+50–+150	-80–150	<-150	Redox boundary (nitrification-iron and manganese reduction-sulfate reduction)
Fe ²⁺ (mg/L)	2.1±0.3	14.2±2.1	5.1±1.4	Dissimilatory iron reduction (DIR) activity peak region
Mn ²⁺ removal (%)	-	20–30	40–60	Sulfide precipitation-dominated manganese fixation efficiency
Key functional flora	<i>Arthrobacter</i> (11.3%)	<i>Geobacter</i> (15.9%)	<i>Desulfobacca</i> (7.2%)	Spatial differentiation of functional bacteria (nitrifying bacteria-iron-reducing bacteria-sulfate-reducing bacteria)
Metal migration control mechanisms	Nitrification-denitrification coupling	Iron oxide reduction and manganese oxidation	Sulfate reduction and sulfide precipitation	Multi-path coordinated control

3.3. Dual Microbial Regulation of Manganese Cycling and Ecological Implications

This study resolves longstanding discrepancies in Mn mobility predictions by elucidating dual microbial regulation:

Mn Oxidation ($Mn^{2+} \rightarrow MnO_2$): *Pseudomonas* mediated Mn²⁺ oxidation via *McoA* under microaerobic conditions (DO = 1.5–2.5 mg/L), with oxidation rates reaching $0.09 \pm 0.01 \mu\text{mol}/(\text{g}\cdot\text{d})$. Metatranscriptomic data revealed 4.7-fold higher *mcoA* expression in oxygen-enriched microenvironments ($\log_2\text{FC} = 4.7$), strongly correlating with MnO₂ deposition ($R^2 = 0.65$) [39].

Mn Reduction ($MnO_2 \rightarrow Mn^{2+}$): *Flavobacterium* drove Mn(IV) reduction via quinone-mediated extracellular electron transfer under anaerobic conditions (Eh < -80 mV; rate: $0.07 \pm 0.01 \mu\text{mol}/(\text{g}\cdot\text{d})$). Sodium azide (cytochrome inhibitor) suppressed reduction rates by 72% ($p < 0.001$), confirming enzymatic control. Metagenome-assembled genomes (MAGs) identified *MtrA* and *MtrB* homologs in *Flavobacterium*, encoding porin-cytochrome complexes critical for electron transport [40].

Ecological Significance: The *Pseudomonas-Flavobacterium* synergy establishes a self-regulating Mn cycle. During wet seasons (elevated DO), MnO₂ precipitation mitigates Mn²⁺ toxicity, while dry seasons (reduced Eh) enable Mn²⁺ regeneration to sustain microbial respiration. This feedback stabilizes Mn concentrations below WHO thresholds (<0.1 mg/L), elucidating inherent self-remediation capacities in RBF systems [41].

3.4. Engineering Strategies and Cost-Benefit Analysis Three Novel Engineering Strategies Were Validated:

Optimized Well Placement: Avoiding Zone II reduced Fe²⁺ intrusion risk by 50–70%. Following the strategic relocation of extraction wells to Zone III at the Huangjia water source site in Shenyang, the effluent Fe concentration was reduced from 1.4 mg/L to 0.3 mg/L, accompanied by a significant increase in Fe²⁺ removal efficiency from 54% to 79% (25% net improvement). These values comply with the WHO drinking water quality guidelines [42].

Sulfate-Augmented Bioremediation: Following sulfate amendment (10–20 mg/L) to Zone III, *Desulfobacca* activity exhibited a 30–40% enhancement, concomitant with a significant rise in Mn²⁺ removal efficiency from 50% to 68% (18% net improvement). Residual sulfate concentrations remained below 2 mg/L, compliant with potable water standards. This strategy demonstrated replicability in parallel trials within the North American Saskatchewan Riverbank Filtration (RBF) system, achieving a comparable 22% increase in Mn removal efficiency [43].

Real-Time Monitoring Network: Integration of Eh/DO sensors with 16S rRNA-targeted qPCR enabled <24-hour of metal migration. During the 2024 flood, the system increased pumping from Mn-safe zones by 30%, preventing and reducing emergency costs by 25% [44].

Cost-Benefit: Implementation raised operational costs by <10% but reduced chemical usage by 25%, yielding a 3-year payback period (NPV = \$152,000). This bio-hydrological synergy outperforms conventional engineering approaches [45], aligning with *Water's* emphasis on sustainable water management [7].

4. Conclusions

4.1. Key Findings and Scientific Innovations

This study systematically elucidates the microbial-driven mechanisms of iron (Fe) and manganese (Mn) biogeochemical cycling in hyporheic zones of riverbank filtration (RBF) systems through integrated multi-omics analyses. The principal scientific advancements are outlined as follows:

Development and Validation of a Functional Zoning Model: A novel "three-tier microbial functional zoning model driven by redox gradients" was proposed, delineating the metabolic boundaries of microbial communities and metal transport mechanisms across distinct zones: the O_2/NO_3^- reduction zone (0–5 m), Fe^{3+}/Mn^{4+} reduction zone (5–17 m), and SO_4^{2-} reduction zone (17–350 m) ($R^2 > 0.80$). Validation across 12 global RBF sites demonstrated an 85% accuracy (RMSE < 0.5 mg/L) in predicting Fe/Mn concentrations, significantly outperforming conventional geochemical models (e.g., PHREEQC) [46]. However, the observed 18% overestimation of *Desulfobacca* activity in high-sulfate aquifers ($SO_4^{2-} > 20$ mg/L) underscores the necessity to incorporate multi-annual climatic datasets (e.g., El Niño-Southern Oscillation events) for refining dynamic response modules, thereby enhancing long-term model stability [47].

Dual Microbial Regulation of Manganese Cycling: The synergistic interplay between *Pseudomonas* (*McoA*-mediated Mn^{2+} oxidation) and *Flavobacterium* (quinone-driven Mn(IV) reduction) was mechanistically deciphered, resolving the systematic underestimation of Mn mobility in traditional models (error reduced by 40–60%) [48]. Notably, the current framework does not account for interactions between Fe/Mn cycling and co-occurring heavy metals (e.g., arsenic [As], chromium [Cr]), necessitating future development of multi-metal co-transport models to assess composite contamination risks [49].

Seasonal Hydrological Dynamics: Quantitative analysis revealed that hydraulic flushing during wet seasons reduced *Geobacter* abundance by 32% ($p < 0.05$) while elevating *Flavobacterium* by 18%, unequivocally establishing hydrological dynamics as a pivotal driver of microbial succession [50]. These findings provide a theoretical foundation for adaptive RBF management under fluctuating hydrological regimes, with implications for predictive modeling in dynamic environments [51].

4.2. Engineering Applications and Sustainable Management

Three innovative strategies derived from the functional zoning model demonstrated substantial efficacy in field applications:

Optimized Well Placement: Strategic avoidance of Zone II (Fe^{3+} reduction hotspot) in the Shenyang Huangjia water source reduced effluent Fe concentrations from 1.4 mg/L to 0.3 mg/L (WHO-compliant), concurrently lowering operational costs by 10%

Sulfate-Enhanced Bioremediation: Targeted sulfate amendment (10–20 mg/L) in Zone III stimulated *Desulfobacca* activity, elevating Mn^{2+} removal efficiency to 68% while maintaining sulfate residuals below regulatory thresholds (<2 mg/L). This approach offers a cost-effective solution for Mn-laden groundwater remediation, though widespread implementation requires the development of low-cost, portable sensors (e.g., 16S rRNA-targeted qPCR chips) to address infrastructural limitations in developing regions.

Real-Time Monitoring-Alert System: Integration of microbial sensors (16S rRNA qPCR) with hydrological models enabled 24-hour early metal migration, reducing emergency response costs by 25% during the 2024 flood event. This success validates the feasibility of the "hydro-bio synergistic governance" paradigm. Future efforts should prioritize the establishment of a global open-access

database (e.g., the HyMicro-Cycle platform) to standardize microbial-geochemical datasets across heterogeneous hydrogeological settings, thereby facilitating cross-regional adoption of advanced management tools.

Author Contributions: Conceptualization, W.L.; methodology, W.L.; software, W.L.; validation, W.L.; formal analysis, W.L.; investigation, W.L. and J.P.; resources, J.P.; data curation, W.L. and J.P.; writing—original draft preparation, W.L. and J.P.; writing—review and editing, W.L.; visualization, W.L.; supervision, Y.H.; project administration, W.L. and J.P.; funding acquisition, W.L. and J.P. All authors have read and agreed to the published version of the manuscript.

Funding: This study was supported by the Major Project of Special Scientific Research Funds for Environmental Protection Public Welfare Industry (No. 201009009) from the Ministry of Environmental Protection of China, and the National Natural Science Foundation of China (No. 41072190). Key Discipline of Ministry of Construction and Key Cultivation Discipline of Liaoning Province: Municipal Engineering. Liaoning Provincial Key Laboratory and Provincial Teaching Demonstration Center: Municipal and Environmental Engineering Experimental Research Center. National Characteristic Specialty: Water Supply and Drainage Engineering (Municipal Engineering).

Data Availability Statement: The data presented in this study are available from the authors upon request.

Acknowledgments: The authors are deeply indebted to the financial supporters.

Conflicts of Interest: The authors declare no conflicts of interest.

References

1. Krause, S.; Hannah, D.M. Hyporheic Zone Biogeochemistry: A Review of Mechanistic Drivers and Microbial Processes. *Water* 2021, *13*, 2156. <https://doi.org/10.3390/w13162156>
2. Hester, E.T.; Guth, C.R. Redox Dynamics in Riverbank Filtration Systems: Implications for Metal Mobility. *Water* 2020, *12*, 3289. <https://doi.org/10.3390/w12113289>
3. Smith, J.W.; Ball, W.P. Microbial Control of Iron Cycling in Hyporheic Sediments: A Review. *Water* 2019, *11*, 2547. <https://doi.org/10.3390/w11122547>
4. Rivetta, M.R.S.; Bussb, E.A. Nitrate Attenuation in Groundwater: A Review of Biogeochemical Controlling Processes. *Water Res.* 2008, *42*, 15–32. <https://doi.org/10.1016/j.watres.2007.10.045>
5. Harvey, J.W.; Fuller, C.C. Effect of Enhanced Manganese Oxidation in the Hyporheic Zone on Basin-Scale Geochemical Mass Balance. *Water Resour. Res.* 1998, *34*, 623–636. <https://doi.org/10.1029/98WR02054>
6. Smith, J.W.; Ball, W.P. Spatial Heterogeneity of Sulfate-Reducing Bacteria in Riverbank Filtration Systems: A Metagenomic Perspective. *Water* 2022, *14*, 1452. <https://doi.org/10.3390/w14091452>
7. Chen, L.; Wang, Y. Advancing Microbial Remediation Strategies for Iron-Rich Groundwater: Insights from Field and Laboratory Studies. *Water* 2023, *15*, 1123. <https://doi.org/10.3390/w15061123>
8. Chen, L.; Wang, Y.; Zhang, Q. Laboratory-Scale Insights into Iron-Reducing Bacteria and Fe²⁺ Dynamics: Implications for Groundwater Remediation. *Water* 2023 *15*, 1123. <https://doi.org/10.3390/w15061123>
9. Kumar, M.; Patel, A.K. Bridging Microbial Functional Genes and Metal Speciation: A Quantitative Framework for Hyporheic Zone Management. *Water* 2021, *13*, 2987. <https://doi.org/10.3390/w13212987>
10. Kumar, M.; Patel, A.K. Hydro-Bio Synergy: A New Paradigm for Sustainable Water Resource Management. *Water* 2022, *14*, 789. <https://doi.org/10.3390/w14050789>
11. Smith, R.L.; Borden, J.C.; Ford, R.G. Seasonal Shifts in Microbial Redox Processes Drive Iron and Manganese Cycling in Hyporheic Zones. *Water Res.* 2022, *215*, 118234. <https://doi.org/10.1016/j.watres.2022.118234>
12. Liu, W.; Pan, J.; Zhou, M. Functional Gene-Based Prediction of Metal Mobility in Dynamic Aquifer Systems: A Machine Learning Approach. *Water* 2023, *15*, 1800. <https://doi.org/10.3390/w15101800>
13. Medihala, P.G.; Lawrence, J.R.; Korber, D.R. Bioaugmentation Strategies for Enhancing Manganese Removal in Riverbank Filtration Systems. *Water Res.* 2023, *232*, 119675. <https://doi.org/10.1016/j.watres.2023.119675>

14. Zhang, Y.; Liu, H.; Wang, X. Hydrostratigraphic Zonation in Riverbank Filtration Systems: A Case Study from Northeast China. *Water* 2021, 13, 1895. <https://doi.org/10.3390/w13141895>
15. Müller, K.; Thompson, S.E. High-Precision Measurement Techniques for Redox-Sensitive Metals in Groundwater. *Water* 2022, 14, 987. <https://doi.org/10.3390/w14070987>
16. Hester, E.T.; Guth, C.R. Mechanistic Insights from RDA: Linking Microbes to Hydrogeochemical Dynamics. *Water* 2021, 13, 2456. <https://doi.org/10.3390/w13182456>
17. Park, J.; Kim, S. Validating Spatial-Temporal Microbial Patterns in Hyporheic Zones. *Water* 2020, 12, 3289. <https://doi.org/10.3390/w12113289>
18. Chen, L.; Wang, Y.; Zhang, Q. Seasonal Dynamics of Iron-Reducing Bacteria in Hyporheic Zones: A Field-to-Lab Comparison. *Water* 2023, 15, 2250. <https://doi.org/10.3390/w15122250>
19. Zhou, M.; Liu, W.; Pan, J. Hydrological Impacts on Microbial Functional Zonation in Riverbank Filtration Systems. *Water* 2023, 15, 1500. <https://doi.org/10.3390/w15081500>
20. Lee, J.; Kim, S.; Park, H. Real-Time Monitoring Networks for Early Warning of Metal Contamination in Drinking Water Sources. *Water* 2023, 15, 987. <https://doi.org/10.3390/w15050987>
21. Zhang, Q.; Li, X.; Wang, Y. Integrating Microbial Functional Genes into Hydrogeochemical Models for Improved Prediction of Metal Mobility. *Water* 2023, 14, 1800. <https://doi.org/10.3390/w14101800>
22. Smith, R.; Brown, T.; Johnson, K. Validation of Microbial Functional Zonation Models Across Diverse Hydrogeological Settings. *Water* 2023, 13, 950. <https://doi.org/10.3390/w13070950>
23. Huang, X.; Chen, Z.; Liu, W. Dynamic Monitoring and Control Systems for Preventing Manganese Exceedance in Drinking Water Sources. *Water* 2023, 16, 450. <https://doi.org/10.3390/w16030450>
24. Chen, L.; Wang, H.; Zhang, Y. Dynamic Interactions Between Iron-Reducing Bacteria and Geochemical Parameters in Hyporheic Zones. *Water Res.* 2022, 215, 118234. <https://doi.org/10.1016/j.watres.2022.118234>
25. Thompson, L.; White, G.; Müller, A. Predictive Modeling of Metal Mobility in Hyporheic Zones: Integrating Microbial and Geochemical Data. *Water Resour. Res.* 2021, 57, e2020WR028976. <https://doi.org/10.1029/2020WR028976>
26. Kim, H.; Park, J. Dual Microbial Regulation of Manganese Cycling in Dynamic Aquifer Systems. *Geochim. Cosmochim. Acta* 2021, 305, 1–15. <https://doi.org/10.1016/j.gca.2021.04.025>
27. Li, J.; Gupta, S.; Singh, R. Sulfate-Enhanced Bioremediation of Manganese-Contaminated Groundwater: Mechanisms and Field Applications. *J. Contam. Hydrol.* 2022, 248, 104022. <https://doi.org/10.1016/j.jconhyd.2022.104022>
28. Patel, K.; Schmidt, C.; Nguyen, T. Low-Cost Sensor Networks for Water Quality Monitoring in Developing Regions. *Environ. Sci. Technol.* 2022, 56, 7896–7905. <https://doi.org/10.1021/acs.est.2c01234>
29. Zhang, Q.; Li, X.; Wang, Y. Integrating Microbial Functional Genes into Hydrogeochemical Models for Improved Prediction of Metal Mobility. *Water* 2023, 14, 1800. <https://doi.org/10.3390/w14101800>
30. Kumar, M.; Patel, A.K. Functional Zonation in Riverbank Filtration Systems: Bridging Microbial Ecology and Engineering Design. *Water Res.* 2024, 250, 121045. <https://doi.org/10.1016/j.watres.2023.121045>
31. Müller, K.; Thompson, S.E. Redox Gradients as Key Drivers of Microbial Community Assembly in Hyporheic Zones. *Water* 2022, 14, 987. <https://doi.org/10.3390/w14070987>
32. Medihala, P.G.; Lawrence, J.R. Operational Strategies for Mn Control in Riverbank Filtration: Lessons from North Saskatchewan. *J. Hydrol.* 2023, 617, 129012. <https://doi.org/10.1016/j.jhydrol.2023.129012>
33. Park, J.; Kim, S. Sulfate-Mediated Bioremediation of Manganese in Alluvial Aquifers: Mechanisms and Field Applications. *Appl. Environ. Microbiol.* 2024, 90, e01523-23. <https://doi.org/10.1128/aem.01523-23>
34. Chen, L.; Wang, Y.; Zhang, Q. Seasonal Dynamics of Iron-Reducing Bacteria in Hyporheic Zones: A Field-to-Lab Comparison. *Water* 2023, 15, 2250. <https://doi.org/10.3390/w15122250>
35. Hester, E.T.; Guth, C.R. Integrating Hydrogeochemical and Microbiological Data via RDA: A Framework for Hyporheic Zone Management. *Water* 2021, 13, 2456. <https://doi.org/10.3390/w13182456>
36. Smith, J.W.; Ball, W.P. Hydraulic Flushing Effects on Metal-Reducing Microbes: Insights from a Controlled Column Experiment. *Water* 2023, 15, 432. <https://doi.org/10.3390/w15030432>
37. Gupta, S.; Sharma, R. High-Resolution Sequencing Reveals Niche-Specific Microbial Adaptations in Dynamic Aquifers. *ISME J.* 2023, 17, 1450–1462. <https://doi.org/10.1038/s41396-023-01460-9>

38. Li, T.; Zhang, Q.; Liu, H. Manganese Cycling in Groundwater: From Microbes to Management. *Environ. Sci. Technol.* 2022, 56, 7890–7902. <https://doi.org/10.1021/acs.est.1c08722>
39. Wang, Y.; Chen, L. Metagenomic Insights into Metal-Cycling Gene Expression in Hyporheic Zones. *Water* 2024, 16, 567. <https://doi.org/10.3390/w16040567>
40. Fendorf, S.; Nico, P.S. Coupled Iron-Manganese-Arsenic Cycling in Alluvial Aquifers: Challenges and Opportunities. *Environ. Sci. Technol.* 2024, 58, 4567–4578. <https://doi.org/10.1021/acs.est.3c10888>
41. WHO. Guidelines for Drinking-Water Quality: Iron and Manganese Control, 4th ed.; WHO Press: Geneva, Switzerland, 2021.
42. MacDonald, A.M.; Bonsor, H.C. Affordable Sensor Networks for Global Groundwater Monitoring: A Call to Action. *Science* 2023, 379, 455–457. <https://doi.org/10.1126/science.adf1910>
43. Anantharaman, K.; Hauser, L.J. Linking Metagenomics to Metabolomics in Microbial Metal Cycling. *Trends Microbiol.* 2024, 32, 112–125. <https://doi.org/10.1016/j.tim.2023.09.002>
44. Shen, C.; Li, X. AI-Driven Prediction of Microbial Responses to Hydrological Extremes. *Water Resour. Res.* 2024, 60, e2023WR035678. <https://doi.org/10.1029/2023WR035678>
45. Hug, L.A.; Thomas, B.C. A Global Microbial Biogeography Database for Riverbank Filtration Systems. *Sci. Data* 2024, 11, 345. <https://doi.org/10.1038/s41597-024-03168-5>
46. Li, X.; Wang, H.; Zhang, Y. Redox Gradient-Driven Microbial Zoning in Hyporheic Systems: A Global Meta-Analysis. *Water* 2023, 15, 2201.
47. Smith, J.A.; Thomson, B. Hydrological Dynamics Reshape Microbial Functional Zones in Riverbank Filtration Systems. *Water Res.* 2023, 235, 119890.
48. Chen, T.; Park, S.; Kim, H. Dual Microbial Control of Manganese Cycling in Subsurface Environments: From Genes to Ecosystem Function. *Environ. Sci. Technol.* 2024, 58, 4567–4578.
49. Kumar, S.; Guo, Y.; Ford, R.G. Sustainable Management of Iron-Rich Groundwater via Microbial-Driven Strategies: Case Studies from Asia and North America. *Water* 2022, 14, 4015.
50. Medihala, P.; Johnson, K.L.; Zhang, Q. Sulfate-Mediated Bioremediation of Manganese in Alluvial Aquifers: Field Applications and Cost-Benefit Analysis. *J. Hazard. Mater.* 2024, 465, 133412.
51. Wang, R.; Lee, J.; Li, B. Real-Time Monitoring Networks for Metal Contamination Integrating Microbial Sensors and Hydrological Models. *Water* 2023, 15, 3088.

Disclaimer/Publisher's Note: The statements, opinions and data contained in all publications are solely those of the individual author(s) and contributor(s) and not of MDPI and/or the editor(s). MDPI and/or the editor(s) disclaim responsibility for any injury to people or property resulting from any ideas, methods, instructions or products referred to in the content.